International Journal of Thermophysics, Vol. 24, No. 3, May 2003 (© 2003)

Experimental and Numerical Investigations of Heat and Mass Transport in Laser-Induced Modification of Ceramic Surfaces[1]

U. Duitsch,[2] S. Schreck,[2] and M. Rohde[2,3]

A laser supported process has been developed to modify the electrical and thermal properties of ceramic substrates locally. This process is characterized by a strong thermal interaction between the laser beam and the ceramic surface which leads to localized melting. During the dynamic melting process, an additional metallic material is introduced. After the solidification, a metal-ceramic composite has been generated with different physical properties compared to the non-modified ceramic. The heat and mass transfer during this dynamic melting and solidification process has been studied experimentally and also numerically in order to identify the dominating process parameters.

KEY WORDS: laser-surface interaction; Marangoni convection; phase change.

1. INTRODUCTION

Ceramic materials are often used as substrates in microelectronics or sensor technologies as carrier boards for active elements. In general, these materials have good dielectric and mechanical properties. However, for specific applications the thermal conductivity of the commonly used ceramic substrates are too low which can lead to high temperature gradients and localized mechanical stresses under heat load. Therefore, in order to overcome these disadvantages, different methods can be applied to modify the thermal and electrical properties on a local scale. We report

[1] Paper presented at the Sixteenth European Conference on Thermophysical Properties, September 1–4, 2002, London, United Kingdom.

[2] Forschungszentrum Karlsruhe GmbH, Institute for Materials Research I, Hermann-von-Helmholtz-Platz 1, D-76344 Eggenstein-Leopoldshafen, Germany.

[3] To whom correspondence should be addressed. E-mail: magnus.rohde@imf.fzk.de

0195-928X/03/0500-0731/0 © 2003 Plenum Publishing Corporation

within this paper on the development of a laser supported process which allows for the fabrication of thermally and electrically conducting lines on ceramic surfaces with a free design (i.e., without using masks) and good mechanical and thermal coupling to the ceramic substrates. Since the thermophysical properties determine the temperature field during the laser-surface interaction, the thermal diffusivity and specific heat have been measured over a wide temperature range. These data have been subsequently introduced into a model which was developed to study the heat and mass transfer during the process.

2. EXPERIMENTAL

The principle of the process is shown in Fig. 1. The laser beam of a high-power CO_2 laser is used to heat the surface of the ceramic above the melting point. Metallic particles are introduced into the localized melt pool. After the solidification a metal-ceramic composite has been generated within the laser irradiated trace. This can be achieved by using a one- or two-step process (see Fig. 1). During the laser process, the ceramic substrate is heated to avoid thermally induced cracking. In order to generate conducting lines, the substrate is moved relative to the laser position with a constant velocity. For most experiments a CO_2 laser ($\lambda_{CO_2} = 10.6\ \mu m$) with a maximum power of 500 W was used. The laser beam was focused to a minimum spot size of about 250 μm. Smaller spot sizes and consequently narrower conducting lines could be achieved by using a Nd:YAG laser ($\lambda_{Nd:YAG} = 1.06\ \mu m$). The laser power was varied between 5 and 50 W. The travelling velocity of the laser or the substrate was adjusted between 500 and 1000 $mm \cdot min^{-1}$. Different ceramic materials were used in the experiments: Al_2O_3 as a reference material, cordierite ($2MgO \cdot 2Al_2O_3 \cdot 5SiO_2$) [1], and the glass ceramics LTCC (low temperature co-fired ceramics). In

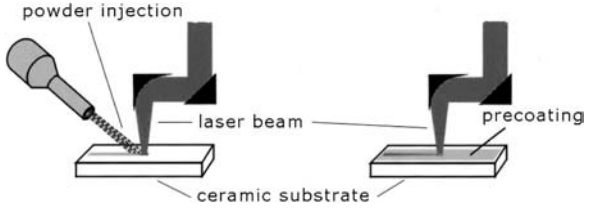

Fig. 1. Schematic of the laser-induced surface modification. One-step process (left): Particles are injected into the melt pool through a nozzle during the laser process. Two-step process (right): A coating of metallic particles are applied prior to the laser process.

the present study particles of different powders (TiC, WC, and W) were added during the laser-induced remelting process.

In order to understand the heat and mass transport during the dynamic melting and solidification and also to optimize the process parameters, different characterization methods were applied to the ceramic materials before, during, and after the laser-induced modification process. The thermophysical properties of the ceramic substrates were characterized using standard measurement techniques: the thermal diffusivity was measured by a laser flash method, the specific heat by differential scanning calorimetry (DSC), and the thermal expansion by a differential push rod dilatometer over a wide temperature range. During the laser process a thermal-imaging system was used to monitor the transient temperature distribution and the heat flow on the ceramic surface. Microstructures of the obtained conducting lines were studied by light and scanning electron microscopy (SEM), and the modified chemical composition was qualitatively analyzed by energy dispersive x-rays (EDX). The electrical conductivity was determined by a standard two-point measurement technique. The local changes of the thermal conductivity were measured with the photothermal method [2]. This method uses an intensity modulated laser beam to induce localized temperature oscillations on the surface of a sample. The amplitude and the phase shift of the oscillating temperature measured by an infrared detector can be used to calculate local changes of the thermal conductivity. By scanning the laser across the surface, a thermal conductivity map can be generated.

3. NUMERICAL METHOD

Besides the experimental investigations, numerical computations have also been performed on the basis of a finite element model (FEM) in order to get more insight into the heat and particle transport during melting and solidification. As an extension of former FEM computations [3] which have only considered the transient temperature distribution and heat diffusion within the solid ceramic to predict the thermally induced mechanical stresses the model was further developed to include the liquid-solid phase change and the heat transport due to convection within the molten pool.

The multi-physics FE-software FEMLAB [4], which is a finite element add-on for the technical computing software MATLAB [5], has been used to solve the Navier–Stokes equations which describe the fluid flow within the melt pool due to the surface tension gradient (Marangoni convection) which is induced by the localized heat source travelling with a constant speed. The heat source is generated by a focused laser beam with a Gaussian-shaped intensity profile which superimposes a strong transient

temperature gradient on the surface. Temperature-dependent material properties like the thermal conductivity and the heat capacity have been included in the model. The computation has been performed under the assumption that the flow is laminar, the fluid is incompressible with a flat free surface, and the Boussinesq approximation has been used to introduce volume forces due to gravitation, which can induce buoyancy effects within the melt. The assumption of a flat free surface instead of a deformed surface of the melt pool leads only to small deviations in the calculated flow field [6]. However, this option has to be included in a further extension of the model. For the modeling of the process a constant value of the density has been used for the solid phase (i.e., at temperatures below the melting point), whereas a temperature-dependent value has been applied for the density within the liquid phase according to

$$\rho(T) = \rho_0(1-\beta(T-T_M)) \qquad \text{for} \quad T > T_M \tag{1}$$

where ρ_0 is the constant density value in the solid phase and β is the volumetric thermal expansion coefficient.

The governing Navier–Stokes equations for the numerical modeling of the process are:

$$\text{continuity} \qquad \frac{\partial(\rho u)}{\partial x}+\frac{\partial(\rho v)}{\partial y}=0 \tag{2}$$

$$x\text{-momentum} \qquad \frac{\partial u}{\partial t}+u\,\nabla u=\frac{1}{\rho}\frac{\partial P}{\partial x}+\mu\,\Delta u \tag{3}$$

$$y\text{-momentum} \qquad \frac{\partial v}{\partial t}+v\,\nabla v=\frac{1}{\rho}\frac{\partial P}{\partial x}+\mu\,\Delta v-g\beta(T-T_M) \tag{4}$$

$$\text{energy} \qquad \frac{\partial T}{\partial t}+u\frac{\partial T}{\partial x}+v\frac{\partial T}{\partial y}=\kappa\,\Delta T \tag{5}$$

with the boundary conditions at the surface at $y = 0$,

$$v=0 \tag{6}$$

$$\mu\frac{\partial v}{\partial y}=-\frac{\partial\sigma}{\partial T}\frac{\partial T}{\partial x} \tag{7}$$

$$q=I(t)\,e^{-\left(\frac{x-x_0}{f}\right)^2} \tag{8}$$

where u and v are the x- and y-velocity components, respectively, t, x, y are the time and space coordinates in the 2D-model, T is the temperature, P is the pressure, ρ is the density of the material, μ is the viscosity, k is the thermal diffusivity, g is the gravitational constant, and T_M is the melting temperature. The boundary conditions given by Eqs. (6)–(8) account for the fact that the y-component of the velocity field vanishes (Eq. (6)) at the free surface, shear forces are generated (Eq. (6)) at the surface of the melt pool due to a gradient in the surface tension σ, and a time-dependent heat flux through the liquid-gas boundary (Eq. (8)) is induced due to the absorption of the laser energy with a Gaussian-shaped intensity profile. Since the laser beam travels with a constant scanning velocity across the surface of the ceramic substrate, the intensity of the heat flux calculated at a given point in space is also a function of time.

The moving melting-solidification boundary and the liquid-solid phase change have been considered in the model by implementing the enthalpy-porosity method [7] into the FE-program. In order to achieve this implementation, additional source terms have been introduced in the momentum (Eqs. (3) and (4)) and energy equation (Eq. (5)) which take in to account that the velocity components vanish in the solid phase and that the enthalpy changes due to the latent heat during the melting process.

For the computation an implicit solver with constant time stepping has been used. The finite element mesh consists of 5952 triangular elements and 3077 nodes, which has been refined in the liquid region, where the flow field and the temperature distribution has to be calculated. In order to achieve grid-independence, it has been evaluated that further refinement does not change the computed results.

4. RESULTS AND DISCUSSION

Typical results of the laser-induced modification process are shown in Fig. 2. The minimum line width which could be achieved with the CO_2 laser system was about 250 μm. With tungsten as an additive material embedded in a cordierite matrix, a specific electrical resistance of the order of $10^{-5}\,\Omega\cdot$m could be obtained. Within these lines an increased thermal conductivity value up to 10 times larger than that for the pure substrate material cordierite could be determined with the photothermal method. A typical result of a photothermal measurement is shown in Fig. 3 which clearly indicates that the thermal conductivity is locally enhanced within the modified line compared to the substrate which is not affected. Using carbide powder as an additional material during the process with a stoichiometric composition like TiC and WC, the local increase in the thermal conductivity is much lower according to even lower thermal conductivity

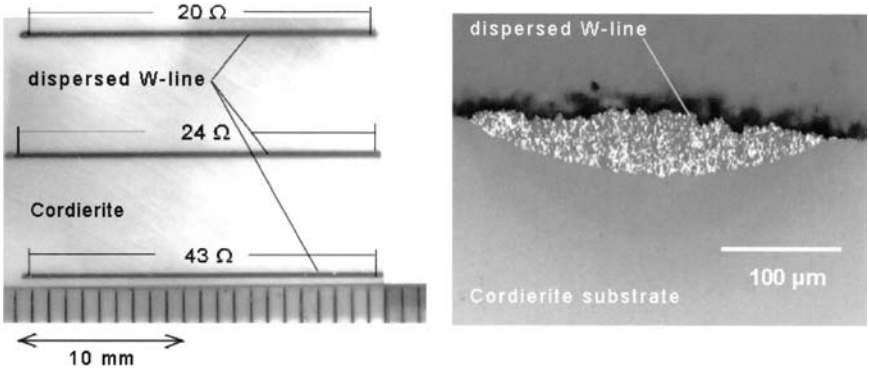

Fig. 2. Electrical resistance of W-lines in cordierite (left) and cross section of the modified area (right).

values of those compounds [8]. With TiC the thermal conductivity within the line could be enhanced by a factor of 1.5 to 2.0 compared to the substrate value whereas this factor amounts to 2.5 to 3.0 using WC.

The results of the temperature dependent measurements (Fig. 4) of the heat capacity and the thermal diffusivity of LTCC and cordierite have been used as a materials database for the model calculations of the heat and

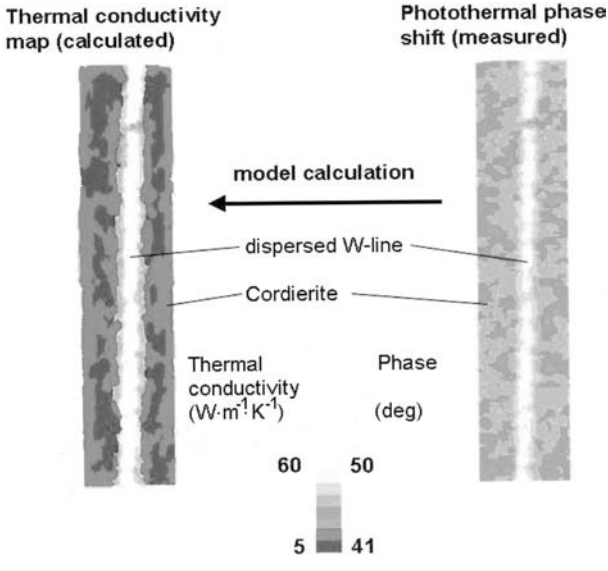

Fig. 3. Result of a photothermal imaging of a W-line in cordierite.

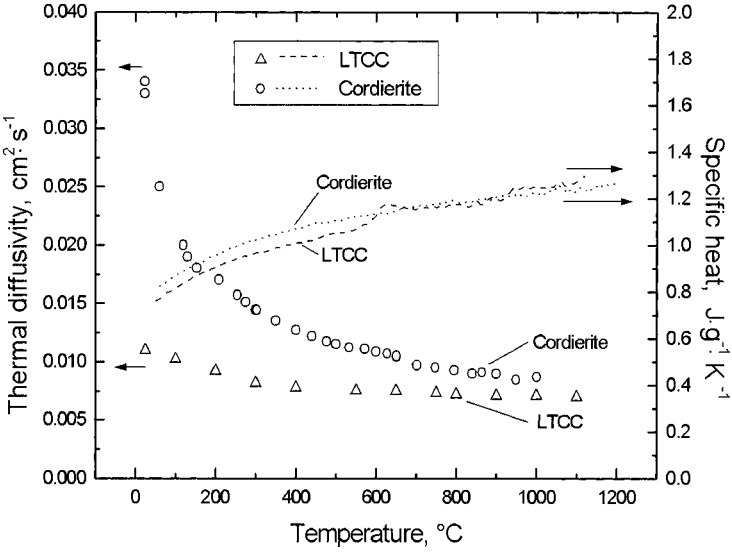

Fig. 4. Measured thermal diffusivity and heat capacity in LTCC and cordierite.

mass transfer during the laser-induced modification process. Within both materials the thermal diffusivity decreases as a function of temperature. The variation of this property over the complete temperature range is stronger in codierite due to the crystalline nature of this ceramic and follows approximately a $1/T$-behavior with increasing temperature. This behavior is not so pronounced in LTCC. Since this material is a multiphase compound [9] with additional glassy phases, internal interfaces and phase boundaries tend to decrease the phonon mean free path and, therefore, reduce the thermal conductivity. The results of the specific heat measurements confirm this interpretation. Compared to the single-phase cordierite, the $c_p(T)$-curve of LTCC shows a broad peak at about 600 and 950°C just before the onset of melting at 1140°C which is much lower than the melting point of cordierite at 1465°C.

The numerical results calculated by the two-dimensional FE-model for the case of the laser-induced remelting of cordierite are shown in Fig. 5 (right). The streamlines within the melt pool, which are frozen in during the solidification, are visible in the cross-sectional microscope image (Fig. 5, left) and can be compared with the predictions of the numerical model. The calculated velocity field within the liquid phase above the melting temperature of cordierite reproduces the influence of shear forces at the surface of the melt pool (Marangoni effect) which induces a convection driven mass

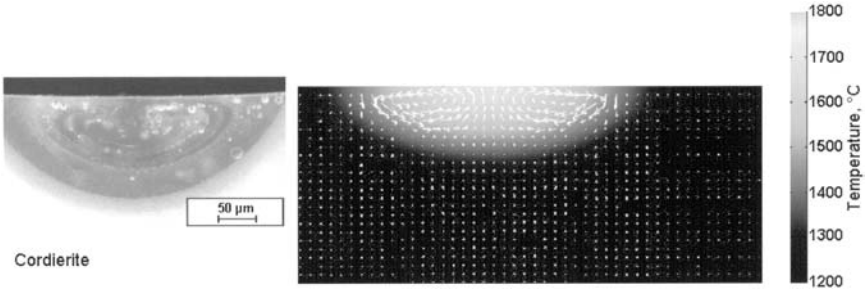

Fig. 5. SEM image of the cross section of a laser melted line (laser power: 7 W, speed: 500 mm · min^{-1}) in cordierite showing the streamlines within the melt pool generated during the process (left). Corresponding temperature and velocity field (right) calculated by the FE model using the same process parameters at a time step of 30 ms after the maximum temperature has been reached.

transport along the negative temperature gradient. For the calculations the volumetric thermal expansion coefficient $\beta = 3.8 \times 10^{-4}\,°C^{-1}$, and the surface tension coefficient $d\sigma/dT = -6 \times 10^{-5}\,kg \cdot s^{-2} \cdot °C^{-1}$ and the viscosity of $\mu = 0.105\,kg \cdot m^{-1} \cdot s^{-1}$ [10] of molten Al_2O_3 have been used in the momentum equation (Eq. (4)) and in the boundary condition (Eq. (7)), respectively, due to the lack of corresponding data for cordierite. The velocity field forced by the temperature dependence of the surface tension leads to a homogeneous distribution of additional materials introduced into the melt pool (see Fig. 2, right) as long as the metal particles do not stick together by sintering effects. By systematic experiments it could be shown that the precoating of cordierite with stoichiometric TiC or WC leads to an infiltration of the cordierite melt into the carbide coating due to capillary forces rather than to mass transport of the metal particles into the melt pool [11].

Experiments on laser surface modification (Fig. 6) show that the mass transport within the melt pool is completely different using LTCC as substrate material compared to cordierite. During the laser-induced remelting, no streamlines due to Marangoni convection can be observed. The lack of surface tension driven convection during the laser process has consequences for the distribution of an additional material introduced into the melt pool. Using a W-precoating during the laser process, the molten ceramic is driven into the porous coating by capillary forces. Since the thermal diffusivity and the specific heat at high temperatures are close to the values of cordierite, the temperature gradient may be also comparable. Since it is known that the surface tension coefficient $d\sigma/dT$ is much lower in glass melts [12] than in liquid metals or ceramics, the absence of the Marangoni convection does not lead to a homogeneous distribution of the metal

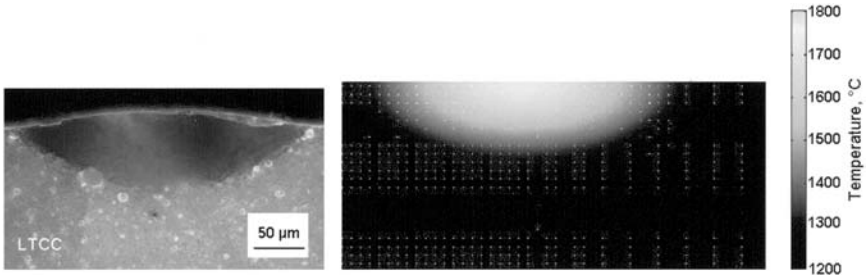

Fig. 6. SEM image of the cross section of a laser melted line in LTCC (laser power: 6 W, speed: 500 mm · min^{-1}) (left). Simulation of the temperature and velocity field by the FE model at the same time step given in Fig. 5 (right).

particles within the ceramic melt pool. The results of the FE simulation, which was computed with a value of $d\sigma/dT = 0$, (Fig. 6, right) reflect this effect, since the calculated maximum value of the velocity field within the LTCC-melt is $v_{max} = 0.06$ mm, which may be due the vanishing surface tension coefficient induced solely by buoyancy forces. For the convection pattern (Fig. 5) in the cordierite melt pool, a maximum value of $v_{max} = 10$ mm · s^{-1} could be calculated. This may be compared with the results of a finite element simulation of a laser process in Al_2O_3 [13], which gives a value of 35 mm · s^{-1} for the maximum velocity at the surface of the molten region.

5. SUMMARY AND CONCLUSION

Laser-supported surface modification of ceramics can be used to produce local changes of the material properties on the surface without affecting the bulk of the ceramic. The interaction of the laser beam with the ceramic leads to strong dynamic temperature gradients which are determined primarily by the thermal diffusivity and the specific heat. The mass transport within the molten ceramic pool depends also on the temperature dependent surface tension at the liquid-gas interface. For substrates precoated with metallic particles like W, or carbide particles like TiC, WC, which do not transform into the molten state, infiltration of the porous coating with the molten ceramic can occur if sintering effects lead to coupling between individual particles.

The results of the studies reported in this paper give some evidence of the fundamental aspects of the transport of heat and mass during laser-induced surface modification of ceramic substrates. However, further systematic experimental studies should be done in order to get more insight into the relationship between the process parameters and the resulting microstructure, composition, and properties of the processed surface. Also,

the numerical model has to be extended in order to include the addition of metals, the surface deformation of the melt pool, and the generation of thermally induced stresses.

REFERENCES

1. S. Rüdiger, H. Gruhn, R. Heidinger, M. Rohde, J. Schneider, and K.-H. Zum Gahr, *Surface Engineering*, EUROMAT 99, Vol. 11, H. Dimigen, ed. (1999), pp. 510–515.
2. M. Rohde, *High Temp.–High Press.* **29**:171 (1997).
3. H. Gruhn, R. Heidinger, M. Rohde, S. Rüdiger, J. Schneider, and K.-H. Zum Gahr, *Proc. MSM 99 Int. Conf. Modeling and Simulation of Microsystems* (1999), pp. 105–108.
4. FEMLAB, *Reference manual*, Version 2.3, COMSOL AB, Stockholm (2002).
5. MATLAB, *Users guide*, Version 6, MATHWORKS Inc., U.S.A. (2000).
6. M. E. Thompson and J. Szekely, *Int. J. Heat Mass Transfer* **32**:1007 (1989).
7. A. D. Brent, V. R. Voller, and K. J. Reid, *Numerical Heat Transfer A* **13**:297 (1998).
8. Y. S. Touloukian, ed., *Thermophysical Properties of Matter, TPRC Data Series*, Vol. 1 (Plenum Press, New York, 1970).
9. A. Dziedzic, L. J. Golonka, J. Kita, and J. M. Kozowksi, *Proc. 24th IMAPS-Poland Conf.* (2000), pp. 163–168.
10. J. L. Bates, C. E. McNeilly, and J. J. Rasmussen, in *Ceramics in Severe Environments*, W. W. Kriegel and H. Palmour, eds. (Plenum Press, New York, 1971), pp. 11–25.
11. S. Schreck, *Thermal and Electrical Conducting Path in Cordierite by Laser-Induced Dispersing Processes Using Hard Particles and Tungsten*, Ph.D. thesis (Universität Karlsruhe, 2002).
12. J. Hlavav, *The Technology of Glass and Ceramics* (Elsevier, Amsterdam, 1983), pp. 78–81.
13. J. W. Hirsch, L. G. Olsen, Z. Nazir, and D. R. Alexander, *Opt. Lasers Eng.* **29**:465 (1998).